Tuning microtubule-based transport via filamentous MAPs: the problem of dynein

Michael Vershinin[†,*], **Jing Xu**[†,*], **David S. Razafsky**[§], **Stephen J. King**[§,+], and **Steven P. Gross**[†,+]

[†]Department of Developmental and Cell Biology, University of California Irvine, Irvine, CA -92612, USA

[§]Division of Molecular Biology and Biochemistry, School of Biological Sciences, University of Missouri-Kansas City, Kansas City, MO 64110, USA

Abstract

We recently proposed that regulating the single-to-multiple motor transition was a likely strategy for regulating kinesin-based transport *in vivo*. Here, we use an *in vitro* bead assay coupled with an optical trap to investigate how this proposed regulatory mechanism affects dynein-based transport. We show that tau's regulation of kinesin function can proceed without interfering with dynein-based transport. Surprisingly, at extremely high tau levels—where kinesin cannot bind microtubules—dynein can still contact microtubules. The difference between tau's effects on kinesin- and dynein-based motility suggests that tau can be used to tune relative amounts of plus-end and minus-end directed transport. As in the case of kinesin, we find that the 3RS isoform of tau is a more potent inhibitor of dynein binding to microtubules. We show that this isoform-specific effect is not due to steric interference of tau's projection domains, but rather due to tau's interactions with the motor at the microtubule surface. Nonetheless, we do observe a modest steric interference effect of tau away from the microtubule and discuss the potential implications of this for molecular motor structure.

Keywords

tau; dynein; kinesin; transport; regulation

Introduction

Microtubule (MT) based transport is crucial for the cells' lifecycle, and is bi-directional. Cargos move from the cell center to periphery via different kinesin-family motors, but transport from the periphery towards the nucleus is achieved almost entirely by cytoplasmic dynein. This microtubule-based transport is heavily regulated (1), so that the right cargos arrive at the right place at the right time. Recent work has suggested that in addition to cargo-based regulation (where regulation alters either the number of cargo-bound motors, or the function of motors that are bound to the cargo), filament-based regulation may play an important role in controlling cargo distributions (2,3). However, work to date has investigated filament-based regulation as a way of tuning plus-end based transport, either to favor transport by specific classes of kinesin motors (4,5), or to control the number of engaged motors to affect MT-MT and MT-actin switching (2). One concern with such

Corresponding author: Steven P. Gross (sgross@uci.edu).
[*]These authors contributed equally to this work.
[+]Co-senior authors.

models is that dynein moves on microtubule tracks just as kinesin does, and might be expected to be affected similarly to kinesin because dynein and kinesin compete for binding to MTs (6). However, this type of regulation of kinesin must be mostly independent from dynein: any alteration of plus-end transport which locally modulates its robustness (2) must nevertheless avoid disrupting the global pattern of dynein-based minus-end transport. Consider for instance the case of axonal transport. Dynein is required for synapse to nuclei communication (7,8) and indeed failure of such communication would be disastrous. Dynein also plays a critical role in the neuronal response to injury, and carries essential signals back to the nucleus to allow the cell to respond appropriately (9). Such damage could come at any time, and the neuron must be able to respond, regardless of its state prior to insult. This need for robust dynein transport raises a key question for filament-level regulation: how can such regulation control plus-end transport, and at the same time allow dynein to function?

Because of the possibility of coupling between opposite motors, and various feedback mechanisms, we chose to investigate this question *in vitro*, where it was possible to unambiguously assess the effects of such filament-level regulation on dynein-based transport. Our past studies focused on the role of different isoforms of the filamentous MT-associated protein (MAP) tau in tuning plus-end transport, predominantly by regulating the number of engaged motors (2). We therefore used this model system to investigate tau's effect on dynein-based transport. Tau is important in its own right (10-12) but is also strongly related to other filamentous MAPs (13), so we expect that lessons from the study of tau's effects will likely qualitatively extend to other MAPs.

Results

Past *in vitro* experiments characterized the function of single motors moving a cargo along an isolated, undecorated microtubule, but now we need to extend this approach to better mimic the *in vivo* situation (14). Specifically, we aimed to investigate the influence of tau on cargos driven by both single and multiple motors. We previously showed that the ensemble function of either kinesin (2) or dynein (15) motors is dramatically different from that of a single motor: in contrast to the ~ 1 micron travel of single motors, *in vitro* cargos are transported many microns along undecorated microtubules. For kinesin-based transport, we previously showed that it is possible to regulate this emergent long-distance transport via the MAP tau even in the absence of any other regulatory factors and pathways.

Here, we employ an *in vitro* bead assay where we can control the number of engaged dynein motors, and can then vary tau concentrations and isoforms. This allows us to isolate and investigate the influence of the longest and the shortest human isoforms of the MAP tau (4RL and 3RS respectively) on ensemble dynein-based transport in terms of dynein's microtubule on-rate and off-rate, as well as force production and velocity. In addition, this controlled environment allows us to explore the potential of tau for down-regulating one direction of transport relative to the other. The design of the present study mirrors our previous kinesin work (2), and the results for both can be directly compared. Briefly, we incubate polystyrene beads with different amounts of bovine cytoplasmic dynein motors, thus varying the average number of motors on beads. By doing so, we can controllably vary the average number of dynein motors participating in cargo transport from one to many. Transport properties described below were measured by bringing cargos pre-incubated with motors near the MTs using an optical trap. Fig. 1a shows a measurement sequence where motor force production, cargo travel distance and velocity were measured. The assay is very robust as it generates negligible optical damage to the motors. Fig. 1b shows that a dynein-driven bead is capable of fast travel even after more than 4 minutes in an optical trap. All data, except Fig. 1a, was obtained at laser power of 28 mW. The data in Fig. 1a was

obtained at lower laser power (8 mW), resulting in more prominent displacement of the bead in the laser trap (compared with Fig. 1b).

To examine the effects of tau on dynein on-rate and travel, independent of its effects on microtubule stability, we employed taxol-stabilized MTs without any tau (hereafter "bare MTs"). We determined the bead-dynein incubation concentration where essentially all beads bound to bare MTs once positioned near them, and measured how far each bead would travel (with optical trap turned off) before attachment at this incubation concentration. Here, the travel was significantly longer range (Fig. 2a,b) than what we and others have reported (15-17) for single dynein motors, indicating that some of the transport in this assay was mediated by multiple dyneins. We then prepared beads at the same incubation concentration, and contrasted our observations with identical experiments but employing taxol stabilized MTs incubated with two distinct tau isoforms (4RL and 3RS). We looked at the effect of 'physiologically relevant' tau concentrations, on dynein-based transport, that is, a range of tau concentrations of the order ~0.1 tau/tubulin dimer that are found in neurons (18). Interestingly, we observed little to no effect of tau on either dynein's on-rate or travel in parallel assays where MTs were incubated with 0.11 of either 4RL (Fig. 2c) or 3RS (Fig. 2d) tau/tubulin dimer. This is in contrast to our previous kinesin study, where this amount of 3RS tau on MTs was sufficient to almost completely inhibit kinesin binding to MTs and thus strongly inhibited kinesin-based cargo travel (2). The 4RL tau did not have as strong an effect on kinesin's on-rate at this concentration, though significant transport inhibition was observed. Therefore, we discover here that under 'normal' tau concentrations, dynein is unaffected, whereas specific tau isoforms can either strongly impair kinesin-based transport or leave it almost unchanged. This finding resolves a fundamental concern with the hypothesis that filament-level regulation may be important for controlling kinesin-based transport, namely that such regulation could have an unintended consequence and impair dynein-based transport. What emerges is the suggestion that additional regulatory pathways are not required for this result, but that instead, somehow the unique molecular architecture of dynein makes it possible for it to be less affected than kinesin by such MAPs.

In order to gain molecular insight into how dynein could avoid being affected, we went to higher concentrations of tau—concentrations above 0.1 tau/tubulin dimer—not usually found in cells. At higher levels (~0.2 tau/tubulin dimer), we found that tau's presence on MTs does begin to affect dynein transport. It is important to note that such high levels of tau essentially completely block kinesin transport, and because kinesin-based transport is required for viability, these levels are not "physiological". The effect (if any) of 4RL tau is very small (Fig. 2e) whereas the effect of 3RS tau is more substantial (Fig. 2f), resulting in single-motor like cargo travel distances. The difference between the effect of 4RL and 3RS tau becomes more pronounced when we increased the amount of dynein on the bead by incubating beads with a dynein concentration approximately four times higher. In fact, even at these high dynein concentrations, the presence of 0.21 tau/tubulin dimer of the 3RS isoform reduced robust long-range transport (Fig. 2g) to short-range single-motor-like motion (Fig. 2i), whereas the 4RL isoform still only had a limited (though significant) effect on dynein travel (Fig. 2h). Together, these results demonstrate that at high enough concentrations of dynein and tau, the effect of tau on dynein-based transport is to reduce mean travel length, and that this effect can depend dramatically on the specific tau isoform.

Given that we were now observing an effect of tau on dynein-based transport, we quantified observed cargo velocities. We note that, as previously reported (15), motion of cargos was not always at uniform velocities. Cargos were observed to change velocity, or exhibited periods of back-and-forth diffusion. We excluded diffusive portions from tracks and parsed the directed motion parts of the tracks into segments of constant velocity (e.g. Fig. 3a) which were then used to construct the distribution histograms for cargos moving on MTs with no

tau, 0.21 of 4RL, and 0.21 of 3RS (Fig. 3b,c,d respectively). We observe no reproducible difference between velocities in any of the three cases. This is consistent with previous reports for dynein velocity in gliding assays in the presence of MAP2 on MTs (19,20). These results suggest that when the motors are already bound to the MT, the tau-motor interaction is not the dominant rate-limiting factor for processive motion. However, this does not imply that tau exclusively affects the dynein on-rate. In fact, we do observe the effect of tau on dynein off-rate as well (see below).

We also measured the maximum force the dynein motors could exert against the optical trap before stalling and subsequently falling back to the center of the optical trap. Our measurements employed beads incubated at the same dynein concentration as those in Fig. 2a-f. The histograms of recorded stall forces in the presence of no tau (Fig. 4a), high levels of 4RL tau (Fig. 4b) and 3RS tau (Fig. 4c) show distinct peaks. The first peak in all three force distributions occurs around 1-1.2 pN. This is in good agreement with our previous report for single cytoplasmic dynein force production on bare MTs (21). This result implies that tau does not alter single dynein's force production, much like it does not alter single kinesin's forces (2).

The force distribution for bare MTs shows three prominent peaks (Fig. 4a) with typical stall lineshapes corresponding to each peak shown in Fig. 4g-i. The peaks are spaced roughly evenly, though we note that the location of the second peak is not quite double that of the first and the third peak occurs at the limit of linear regime of our optical trap. In parallel with our kinesin experiments and following our previous dynein report (15), we ascribe these peaks to contributions from one, two, and three dynein motors respectively. Indeed, contribution from more than one motor in Fig. 4a is expected, since the corresponding cargo travel (Fig. 2a,b) is significantly greater than for the single-motor case (15-17).

The force measurements started to provide insight into how dynein could be affected differently than kinesin. In dynein assays, we find little to no difference between stalling force measurements with no tau and 0.21 4RL tau (Fig. 4a and 4b respectively); cargos are frequently driven by more than one motor. This is in strong contrast to kinesin-based transport, which is almost entirely abolished at 0.21 4RL tau—in the rare instances when it does occur, it is driven only by a single motor (2). Kinesin-based transport is even more thoroughly abolished at 0.21 3RS tau—tau so efficiently blocks the access of the motors to MTs, that we did not see any binding events even for beads from multiple-kinesin assays. This is not the case for dynein: while force production for beads in the presence of 0.21 3RS tau (Fig. 4c) does show a reduction of higher stalling force peaks (which we ascribed to multiple motor activity) relative to the single motor peak, multiple-motor events are still observed. Similarly, confirming the histograms of stalling forces (Fig 4d-e), at high levels of tau, the records of motion in the trap show frequent excursions of motion past 1.5 pN, corresponding to motion driven by at least two motors (Fig 4e,f). While overall frequency of multiple-motor events (larger than 1.5 pN) clearly declines in the 0.21 3RS tau assay (Fig 4f) relative to that of no tau (Fig 4d) and 0.21 4RL tau assays (Fig. 4e), the effect is much less than what would be observed for kinesin where there would be no motion in the 3RS case, and only rare single-motor driven events in the 0.21 4RL case. We conclude that even in the presence of high amounts of tau, dynein can still bind the microutubules; its on rate has been much less effected than for kinesin.

The stronger effect of 0.21 3RS tau seen in force production (Fig. 4c,f) is consistent with the corresponding shorter cargo travel (Fig. 2f). However, the key observation here is that travel length results cannot be simply attributed to tau reducing the average number of actively engaged motors. 3RS tau reduces travel to single motor-like limit, however, the contributions from two and three motors are still apparent in the force distribution histogram

(Fig. 4c). We thus conclude that tau inhibits dynein-based motility via a two-fold mechanism: tau somewhat reduces the number of engaged dynein motors by reducing dynein's on-rate, but equally importantly it substantially affects dynein travel by increasing dynein's off-rate.

Dynein has different dynamics from kinesin: unlike kinesin, it is able to take large steps, switch protofilaments, and reverse course. We wanted to try to separate the importance/ effects of tau on dynein's ability to bind MTs from such potential dynamic effects. To directly address tau's influence on motor on-rate, independent of dynein dynamical function, we decided to look at the effect of tau on the interaction between the MT and the MT-binding domain of dynein. To do this, we took a small GST-tagged recombinant protein fragment of dynein including the MT binding domain, and attached such fragments via anti-GST antibodies to polystyrene beads (see methods), and then examined the effect of the presence of tau on the binding of the beads to MTs. Control experiments showed that beads incubated with just the anti-GST antibody or just the GST-tagged MTBD (but no AB) did not bind to microtubules either spontaneously, or when held near them in an optical trap. When beads with an expected complete linkage (i.e. incubated with both the antibody and the MTBD), were held close, we did observe bead-MT binding. We could tune the binding rate by tuning the incubation concentration of MTBD, and we chose a concentration where ~80% of the beads bound to bare MTs (i.e. MTs with no tau on them). At such high binding rate, we observed many beads bound to MTs without being positioned near them by the trap. The presence of tau on MTs reduced the binding rate significantly (to $15 \pm 5.6\%$ for 0.21 of 3RS tau and $27.5 \pm 7.1\%$ for 0.21 of 4RL tau). This result directly confirms that tau can significantly inhibit dynein's on-rate, independent of dynein's dynamics.

The inhibition of binding by the 3RS tau was stronger than the 4RL tau. Not only was the binding rate lower in the 3RS assay, as reported above, but we also did not observe any spontaneous binding of beads to MTs in that assay. By contrast, very rare spontaneous binding events were observed in the 4RL assay. What is the mechanism for this difference in the inhibitory effect of different tau isoforms? Is it due to tau's steric interference with motor diffusion near the MT or is it due to interactions localized to the MT itself (e.g. modification of local charge environment at or near the motor binding site)? If the steric effect were the dominant factor, then one would expect stronger inhibition of motor binding in the 4RL assay since the projection domain of that isoform is longer. However we observe the exact opposite, strongly arguing against this scenario.

To further investigate this hypothesis—that the differences in tau's effects on dynein are due to local changes in surface chemistry, and not steric effects due to the projection domains— we measured tau's steric inhibition in a geometry maximally similar to the one described above. We used identical protein A beads, but instead of using dynein's MT binding domain, we incubated the beads with an anti-tubulin antibody. Since the geometry in both cases was nearly identical, steric effects of tau were essentially the same in all cases. Therefore, any differences between binding rates could be attributed directly to local effects at the MT surface.

The antibody concentration was again chosen so that the binding fraction of beads to bare MTs was ~80%, the same as for the MTBD assay. We found that the effect of tau on the anti-tubulin antibody binding was significantly smaller than for corresponding MTBD assays (to $60 \pm 15.5\%$ for 0.21 of 3RS tau and $58.3 \pm 14.1\%$ for 0.21 of 4RL tau). Note that the effect of the two isoforms is similar and any difference is not statistically significant, but if anything the effect of 4RL isoform is stronger in agreement with previous reports(22).

Discussion

Our published results for kinesin show that at physiological levels 3RS tau can impair kinesin-based transport but that 4RL tau has a much smaller effect and suggest that this difference can be used to regulate and route plus-end directed traffic. The results presented here for dynein motility in the presence of tau on MTs show that at these tau levels neither isoform significantly hinders dynein transport. In our experiments, we control the overall amount of tau present, but not its distribution along the microtubules. Therefore, at any position along the microtubule the 'local' tau concentration a particular motor sees could be quite different from the average tau value we report (which reflects the global ratio of tau to tubulin dimers). Our experiments represent what happens when tau's binding to MTs is not additionally regulated; regulatory *in vivo* mechanisms likely further modulate tau's distribution and such scenarios are not addressed within the scope of this work.

Tau's interference with transport conceivably arises from two possible mechanisms: steric interference with motors away from the MT surface, or chemical/charge interaction at the MT surface (e.g. local presence of tau modifying motor binding site to make binding less likely). One potential way to distinguish between these mechanisms would be to use truncated constructs of tau (23) with a shorter projection domain or no projection domain at all. Thus, one could hope to remove tau's effects away from the MT while isolating tau's affects at the MT. However, the projection domain of tau is acidic while the rest of the molecule is basic (24), so such constructs feature significant alteration of charge distribution within the tau molecule. However, tau-MT interactions are sensitive to local charge distribution (25) and it is known that different constructs have different MT-binding properties (23). Therefore, we hypothesized that using truncated constructs of tau was unlikely to exclusively affect local geometry and not local chemistry. Thus, instead of modifying tau, we chose to modify the motor side, and attach dynein's MT-binding domain to beads in a known geometry. We then compared binding of this assembly to MTs with and without tau on MTs. We were also able to measure bead-MT attachment rate in minimally modified geometry where binding was due to an anti-tubulin antibody rather than dynein's MT-binding domain. Taken together, these experiments allowed us to decouple steric effects from effects at the MT surface, as described below.

Steric effects

Tau's inhibitory function may come from its steric interference with motors attempting to bind to MTs. Indeed, previous *in vitro* gliding assay studies (26) found that the inhibitory function of tau is significantly reduced for a tau construct lacking the projection domain. Our measurements also show cases of tau's inhibition of binding which are most naturally explained by steric effects. Most notably, consider the binding of protein A beads incubated with anti-tubulin antibody (Fig. 5b). When such beads are held near bare microtubules with an optical trap, they bind at a rate of ~80.0%. However, when the same experiment is performed with microtubules covered with 0.21 3RS or 4RL tau, the binding rate drops to ~60% (Fig. 5c). It is believed that tau's primary binding site is located on α-tubulin (27), so tau is unlikely to inhibit the binding of the β-tubulin antibody (6G7) used here. Therefore we speculate that the drop in binding rate most likely comes from tau's steric inhibition.

It is also important to compare and contrast tau's effect on dynein and kinesin motors. Structurally, there is a fundamental difference between these enzymes. Kinesin's motor domain directly binds the microtubule and is a globular domain (~9 nm thick and 10 nm long (28)). In contrast, dynein reaches the MT via a thin stalk (~2 nm thick and 15.5 nm long (29)). We hypothesize that this long stalk plays a role in dynein's resistance to the effects of fibrous MAPs such as tau. Previously, the reason for dynein's unusual architecture has been unclear. It was suggested (30,31) that because the ATPase domains were large, the

stalk was required to allow the two heads to both reach the microtubule. However, given recent observations that these ATPase domains are relatively flat (29,32), and often observed in a stacked organization in axonemal dyneins (33-35), such a long stalk may not actually be required to accommodate multiple dynein heads binding in close proximity around a MT (36). Instead, relative to kinesin, we hypothesize that the thin dynein stem is optimized to be able to more easily pierce the "wagging wall" of tau projection domains.

The steric effect of MAPs may also be one reason why kinesin holds its cargos ~17 nm away from the MT (37): a vesicle moved by kinesin needs to stay close to the MT to minimize bumping into various obstructions in a dense cellular environment, however not so close that it would experience sizeable drag from the MAPs. It is curious to consider this in the context of dynein motility. Dynein's AAA-ring domain is also potentially subject to drag by MAPs. Though it is much smaller than typical cellular vesicles, this is balanced by the fact that its spacing from the MT is also slightly smaller than that of kinesin cargos: ~15 nm (29). We hypothesize that resistance or sensitivity to MAPs in general, and tau in particular, may be an important contributor to determining the structure of molecular motors.

Binding inhibition at the microtubule

Tau's presence near the motor's MT binding site likely gives rise to local interactions which inhibit motor binding and transport. Such interactions could affect both dynein and kinesin since these motors compete for binding to MTs (26) and thus their binding sites likely overlap. Indeed, we see that both for kinesin and dynein, the 3RS isoform of tau inhibits binding more potently than the 4RL isoform and we show here that this difference can be directly attributed to interactions at the microtubule (rather than away from it).

To isolate tau's effect on motor binding rather than dynamics, we used the dynein MT-binding domain construct fused with a GST tag. We have attached this protein to an anti-GST antibody and incubated this assembly with protein-A beads (Fig 5a). We see a marked difference between the binding of such beads to microtubules with and without tau. The presence of both tau isoforms inhibits binding (Fig. 5c) but 3RS isoform is the more potent inhibitor. Can this be due to steric effects? To rule out this possibility we performed a control experiment using beads with nearly identical surface decoration: protein-A bound to an anti-tubulin antibody. The main difference between the two geometries is the absence of GST-tagged MT-binding domain of dynein. Therefore, the linkage between the bead and the microtubule is shorter in the control case. Hence, the bead needs to get closer to the MT surface to bind to it, and thus this configuration is subject to more steric hindrance. The control experiment therefore provides us with an upper estimate of the steric inhibition. As can be seen from Fig. 5c this inhibition is far less potent than either isoform of tau. Inhibition of kinesin motor activity at the MT-binding site has been observed for MAP2c - a tau family protein (38). Our results therefore suggest that such inhibition is a more general effect for an entire class of MAPs.

Tau's effect on dynein transport

Our work reveals that tau's presence on MTs affects both dynein on-rate and off-rate. First, notice the frequent directed bead movements in Fig. 4d-f. The fact that robust motor activity is seen for high levels of tau on MTs suggests that dynein's on-rate is affected far less than kinesin's (where such events would be either very rare or non-existent). However the effect on dynein's on-rate is unmistakable. First, force production events do become rarer at high levels of tau. Second, at high levels of tau we observe fewer high force events attributable to multiple-motor activity (Fig. 4). We also show the effect of tau on dynein on-rate directly in the protein-A bead assays (see above and Fig. 5) where we isolate dynein's MT-binding domain and show that dynein's MT-binding function is inhibited by tau. All of the above

data suggests that before dynein even "sets foot" on a microtubule it feels tau's inhibitory effect.

We also show (Fig. 2) that once bound to tau-covered MTs, dynein does not move as far as on bare MTs. In fact, in bead assays where stalling force measurements indicate significant multiple-motor activity, we nonetheless see bead travel distances as low as for beads driven by single motors on bare MTs. This can only be explained if tau affects individual dynein motor's off-rates.

We previously proposed (2,14) that tau acts as a local routing agent in two key ways. First, increased amounts of tau known to reside at the distal ends of axons could aid cargo detachment when it is moving from soma to the periphery. Second, tau residing at intersections could help kinesin-driven cargos avoid tug-of-war scenarios by locally reducing the number of engaged kinesin motors. Existing evidence (39) hints that the more potent 3R tau localizes to MT intersections *in vivo*. Such mechanisms would not work if dynein function were equally or more inhibited by tau as kinesin function. Here we show that in fact, dynein is less sensitive to tau than kinesin. Dynein can still bind MTs at levels of tau where kinesin cannot. It also likely has more options than kinesin when it is already moving along a MT and comes across a tau "roadblock". It should be able to reverse course and switch filaments (16) until it finds an alternate route to pass the tau, whereas kinesin would simply wait until the obstacle detaches (40). Dynein may also find it easier to bypass tau by taking larger steps (21). In general, it is curious that many key structural and mechanical features which so starkly distinguish dynein from kinesin motors all conspire to make it a more robust transporter in the face of MAPs.

Our findings that extremely high levels of tau are needed to affect dynein-based transport suggest that tau is unlikely to serve as a local regulator for the number of engaged dynein motors *in vivo*. However, the fact that at levels found in living cells tau can affect kinesin but not dynein transport suggests that in addition to potentially locally regulating kinesin-based filament switching, tau can in principle tune the amount of allowed plus-end transport without affecting minus-end transport. Moderate levels of 4RL tau will leave both directions unaffected, but high levels of 4RL tau will favor minus-end transport over plus-end transport. Even more extreme tuning can be achieved by 3RS tau, which at moderately high levels severely impairs plus-end transport, and at high levels abolishes it. Our *in vitro* study thus helps us understand *in vivo* observations that excess tau in cells affects primarily plus-end directed transport (41,42)– the inhibition of minus end transport likely does occur but is negligible, resulting in no apparent minus-end motion phenotype. No feedback or additional compensatory changes are needed to understand this *in vivo* observation. Our result also further bolsters our speculation regarding the role of excess tau seen in healthy neurons at the distal ends of axons (both in absolute amount and relative to tubulin abundance (43,44)). We now know that excess tau need not inhibit the loading of soma-destined cargos onto MTs yet it can still help unload plus-end directed cargos.

Note: while this paper was in revision, we have learned of a similar effort (45), where the authors come to qualitatively similar conclusions. However, that assay was performed with a dynein-dynactin assembly and so is a more complex scenario than is explored here, particularly since tau and dynactin are known to interact (46).

Materials and Methods

Protein purification

The purification of tau isoforms and tubulin was as previously described (2). Bovine brain cytoplasmic dynein was purified using a nucleotide dependent microtubule affinity

purification protocol (47). In order to maximize the quality of the dynein motor preparations, we compared dynein preparations purified utilizing different buffer conditions. We found that cytoplasmic dynein was most active (defined by the velocity of single motors and the number of days that the motor retained full activity) when purified in pH 6.6 buffers. All dynein motor preparations used in this work were purified in the optimized pH 6.6 buffers.

In Vitro Motility Assay

Microtubules were incubated with tau and fixed to glass slides as previously described (2), so that dynein results presented here can be directly compared with the previously published kinesin observations (2).

Dynein assay was prepared as previously described (15), with the following exceptions. Data recording and analysis were performed as previously described (2).

Binding experiments

We have used 1 μm diameter polystyrene beads conjugated with protein-A (Polysciences, Inc. Warrington, PA). To test the ability of dynein's MT-binding domain to bind to MTs, these beads (0.3 pM) were incubated for 10 minutes at room temperature with saturating amount (0.3 nM) of 05-782 anti-GST antibody (Millipore, Billerica, MA) and the GST-tagged dynein MT-binding domain construct (see below). To test anti-tubulin antibody binding to MTs, the beads were incubated for 10 minutes at room temperature with 6G7 antibody (Developmental Studies Hybridoma Bank, University of Iowa, Iowa City, IA). The amounts of MT-binding domain protein and 6G7 antibody were set so that 80% of beads in the respective assays bound to bare MTs. The beads were admitted into the flow chamber where MTs were already present as described above. Bead binding was tested by bringing the beads close to the MTs with an optical trap. Beads were found to bind to the MTs if they failed to diffuse away from the MTs when the trap was switched off. To avoid possible non-specific binding to the surface we sought out loose MTs and tested binding to those only. Thus, we could gain additional confirmation of bead binding to MTs by visually correlating random motions of the MT and the bead.

MTBD purification

The dynein MT-binding domain fragment was expressed from pGex4T-1 and purified as follows. Bacterial cells were induced with 0.5mM isopropyl-J-D-thiogalactopyranoside for 19h at 25°C and harvested by centrifugation. The cells were resuspended in lysis buffer (35mM Tris-Cl at pH 7.2, 5mM $MgSO_4$, 5mM B-mercaptoethanol, 0.01% Nα-benzoyl-L-arginine methyl ester, 0.01% Nα-4-tosylamino-L-arginine methyl ester, 0.01% L-1-4′ tosylamino-2-phenylethyl chloromethyl ketone with 100 ug ml^{-1} lysozyme) and homogenized by sonication. The cell extract was centrifuged at 12,000g for 15min at 4°C in an SS-34 rotor. The supernatant was clarified by centrifugation at 30,000g for 30min at 4°C in a Ti45 rotor and loaded onto glutathione agarose beads (Sigma) that had been equilibrated in GST column buffer (35mM Tris-Cl at pH 7.2, 5mM $MgSO_4$, 100mM NaCl). The column was washed with GST column buffer and eluted in GST elution buffer (35mM Tris-Cl at pH 7.2, 5mM $MgSO_4$, 100mM NaCl, 10mM reduced glutathione). The peak elution fractions were pooled, loaded onto a HiTrap heparin sepharose column (GE Biosciences, Piscataway, NJ) that had been equilibrated in HepS column buffer (35mM Tris-Cl at pH 7.2, 5mM $MgSO_4$). The protein was eluted in HepS elution buffer (35mM Tris-Cl at pH 7.2, 5mM $MgSO_4$, 350mM NaCl). Protein concentration was determined by the Bradford assay (Biorad, Hercules, CA). Further characterization of the MT binding domain is being published elsewhere.

Supplementary Material

Refer to Web version on PubMed Central for supplementary material.

References

1. Kamal A, Goldstein LS. Connecting vesicle transport to the cytoskeleton. Curr Opin Cell Biol. 2000; 12(4):503–508. [PubMed: 10873823]

2. Vershinin M, Carter BC, Razafsky DS, King SJ, Gross SP. Multiple-motor based transport and its regulation by Tau. Proc Natl Acad Sci U S A. 2007; 104(1):87–92. [PubMed: 17190808]

3. Reed NA, Cai D, Blasius TL, Jih GT, Meyhofer E, Gaertig J, Verhey KJ. Microtubule acetylation promotes kinesin-1 binding and transport. Curr Biol. 2006; 16(21):2166–2172. [PubMed: 17084703]

4. Ikegami K, Heier RL, Taruishi M, Takagi H, Mukai M, Shimma S, Taira S, Hatanaka K, Morone N, Yao I, Campbell PK, Yuasa S, Janke C, Macgregor GR, Setou M. Loss of alpha-tubulin polyglutamylation in ROSA22 mice is associated with abnormal targeting of KIF1A and modulated synaptic function. Proc Natl Acad Sci U S A. 2007; 104(9):3213–3218. [PubMed: 17360631]

5. Rosenbaum J. Cytoskeleton: functions for tubulin modifications at last. Curr Biol. 2000; 10(21):R801–803. [PubMed: 11084355]

6. Mizuno N, Toba S, Edamatsu M, Watai-Nishii J, Hirokawa N, Toyoshima YY, Kikkawa M. Dynein and kinesin share an overlapping microtubule-binding site. Embo J. 2004; 23(13):2459–2467. [PubMed: 15175652]

7. Mackenzie GG, Keen CL, Oteiza PI. Microtubules are required for NF-kappaB nuclear translocation in neuroblastoma IMR-32 cells: modulation by zinc. J Neurochem. 2006; 99(2):402–415. [PubMed: 17029595]

8. Mikenberg I, Widera D, Kaus A, Kaltschmidt B, Kaltschmidt C. Transcription Factor NF-kappaB Is Transported to the Nucleus via Cytoplasmic Dynein/Dynactin Motor Complex in Hippocampal Neurons. PLoS ONE. 2007; 2:e589. [PubMed: 17622342]

9. Hanz S, Fainzilber M. Retrograde signaling in injured nerve--the axon reaction revisited. J Neurochem. 2006; 99(1):13–19. [PubMed: 16899067]

10. Lace GL, Wharton SB, Ince PG. A brief history of tau: the evolving view of the microtubule-associated protein tau in neurodegenerative diseases. Clin Neuropathol. 2007; 26(2):43–58. [PubMed: 17416103]

11. Lee G. Tau and src family tyrosine kinases. Biochim Biophys Acta. 2005; 1739(2-3):323–330. [PubMed: 15615649]

12. Goedert M. Tau protein and neurodegeneration. Semin Cell Dev Biol. 2004; 15(1):45–49. [PubMed: 15036206]

13. Dehmelt L, Halpain S. The MAP2/Tau family of microtubule-associated proteins. Genome Biol. 2005; 6(1):204. [PubMed: 15642108]

14. Gross SP, Vershinin M, Shubeita GT. Cargo transport: two motors are sometimes better than one. Curr Biol. 2007; 17(12):R478–486. [PubMed: 17580082]

15. Mallik R, Petrov D, Lex SA, King SJ, Gross SP. Building complexity: an in vitro study of cytoplasmic dynein with in vivo implications. Curr Biol. 2005; 15(23):2075–2085. [PubMed: 16332532]

16. Wang Z, Khan S, Sheetz MP. Single cytoplasmic dynein molecule movements: characterization and comparison with kinesin. Biophys J. 1995; 69(5):2011–2023. [PubMed: 8580344]

17. King SJ, Schroer TA. Dynactin increases the processivity of the cytoplasmic dynein motor. Nat Cell Biol. 2000; 2(1):20–24. [PubMed: 10620802]

18. Binder LI, Frankfurter A, Rebhun LI. The distribution of tau in the mammalian central nervous system. J Cell Biol. 1985; 101(4):1371–1378. [PubMed: 3930508]

19. Paschal BM, Obar RA, Vallee RB. Interaction of brain cytoplasmic dynein and MAP2 with a common sequence at the C terminus of tubulin. Nature. 1989; 342(6249):569–572. [PubMed: 2531294]

20. Lopez LA, Sheetz MP. Steric inhibition of cytoplasmic dynein and kinesin motility by MAP2. Cell Motil Cytoskeleton. 1993; 24(1):1–16. [PubMed: 8319263]

21. Mallik R, Carter BC, Lex SA, King SJ, Gross SP. Cytoplasmic dynein functions as a gear in response to load. Nature. 2004; 427(6975):649–652. [PubMed: 14961123]

22. Ross, JL. PhD thesis. 2004. Biological Physics Studies of Microtubules, Taxol, and the Microtubule-Associated Protein, Tau.

23. Gustke N, Trinczek B, Biernat J, Mandelkow EM, Mandelkow E. Domains of tau protein and interactions with microtubules. Biochemistry. 1994; 33(32):9511–9522. [PubMed: 8068626]

24. Amos LA, Schlieper D. Microtubules and maps. Adv Protein Chem. 2005; 71:257–298. [PubMed: 16230114]

25. Barghorn S, Zheng-Fischhofer Q, Ackmann M, Biernat J, von Bergen M, Mandelkow EM, Mandelkow E. Structure, microtubule interactions, and paired helical filament aggregation by tau mutants of frontotemporal dementias. Biochemistry. 2000; 39(38):11714–11721. [PubMed: 10995239]

26. Hagiwara H, Yorifuji H, Sato-Yoshitake R, Hirokawa N. Competition between motor molecules (kinesin and cytoplasmic dynein) and fibrous microtubule-associated proteins in binding to microtubules. J Biol Chem. 1994; 269(5):3581–3589. [PubMed: 8106402]

27. Santarella RA, Skiniotis G, Goldie KN, Tittmann P, Gross H, Mandelkow EM, Mandelkow E, Hoenger A. Surface-decoration of microtubules by human tau. J Mol Biol. 2004; 339(3):539–553. [PubMed: 15147841]

28. Hirokawa N, Pfister KK, Yorifuji H, Wagner MC, Brady ST, Bloom GS. Submolecular domains of bovine brain kinesin identified by electron microscopy and monoclonal antibody decoration. Cell. 1989; 56(5):867–878. [PubMed: 2522351]

29. Burgess SA, Walker ML, Sakakibara H, Knight PJ, Oiwa K. Dynein structure and power stroke. Nature. 2003; 421(6924):715–718. [PubMed: 12610617]

30. Gee M, Vallee R. The role of the dynein stalk in cytoplasmic and flagellar motility. Eur Biophys J. 1998; 27(5):466–473. [PubMed: 9760728]

31. Vallee RB, Gee MA. Make room for dynein. Trends Cell Biol. 1998; 8(12):490–494. [PubMed: 9861671]

32. Samso M, Koonce MP. 25 Angstrom resolution structure of a cytoplasmic dynein motor reveals a seven-member planar ring. J Mol Biol. 2004; 340(5):1059–1072. [PubMed: 15236967]

33. Lupetti P, Lanzavecchia S, Mercati D, Cantele F, Dallai R, Mencarelli C. Three-dimensional reconstruction of axonemal outer dynein arms in situ by electron tomography. Cell Motil Cytoskeleton. 2005; 62(2):69–83. [PubMed: 16106450]

34. Nicastro D, McIntosh JR, Baumeister W. D structure of eukaryotic flagella in a quiescent state revealed by cryo-electron tomography. Proc Natl Acad Sci U S A. 2005; 102(44):15889–15894. [PubMed: 16246999]

35. Nicastro D, Schwartz C, Pierson J, Gaudette R, Porter ME, McIntosh JR. The molecular architecture of axonemes revealed by cryoelectron tomography. Science. 2006; 313(5789):944–948. [PubMed: 16917055]

36. Reck-Peterson SL, Yildiz A, Carter AP, Gennerich A, Zhang N, Vale RD. Single-molecule analysis of dynein processivity and stepping behavior. Cell. 2006; 126(2):335–348. [PubMed: 16873064]

37. Kerssemakers J, Howard J, Hess H, Diez S. The distance that kinesin-1 holds its cargo from the microtubule surface measured by fluorescence interference contrast microscopy. Proc Natl Acad Sci U S A. 2006; 103(43):15812–15817. [PubMed: 17035506]

38. Al-Bassam J, Roger B, Halpain S, Milligan RA. Analysis of the weak interactions of ADP-Unc104 and ADP-kinesin with microtubules and their inhibition by MAP2c. Cell Motil Cytoskeleton. 2007; 64(5):377–389. [PubMed: 17326138]

39. Kosaka S, Takuma H, Tomiyama T, Mori H. The distributions of tau short and long isoforms fused with EGFP in cultured cells. Osaka City Med J. 2004; 50(1):19–27. [PubMed: 15646255]

40. Seitz A, Surrey T. Processive movement of single kinesins on crowded microtubules visualized using quantum dots. Embo J. 2006; 25(2):267–277. [PubMed: 16407972]

41. Chee FC, Mudher A, Cuttle MF, Newman TA, MacKay D, Lovestone S, Shepherd D. Over-expression of tau results in defective synaptic transmission in Drosophila neuromuscular junctions. Neurobiol Dis. 2005; 20(3):918–928. [PubMed: 16023860]

42. Ebneth A, Godemann R, Stamer K, Illenberger S, Trinczek B, Mandelkow E. Overexpression of tau protein inhibits kinesin-dependent trafficking of vesicles, mitochondria, and endoplasmic reticulum: implications for Alzheimer's disease. J Cell Biol. 1998; 143(3):777–794. [PubMed: 9813097]

43. Black MM, Slaughter T, Moshiach S, Obrocka M, Fischer I. Tau is enriched on dynamic microtubules in the distal region of growing axons. J Neurosci. 1996; 16(11):3601–3619. [PubMed: 8642405]

44. Kempf M, Clement A, Faissner A, Lee G, Brandt R. Tau binds to the distal axon early in development of polarity in a microtubule- and microfilament-dependent manner. J Neurosci. 1996; 16(18):5583–5592. [PubMed: 8795614]

45. Dixit R, Ross JL, Goldman YE, Holzbaur EL. Differential Regulation of Dynein and Kinesin Motor Proteins by Tau. Science. 2008

46. Magnani E, Fan J, Gasparini L, Golding M, Williams M, Schiavo G, Goedert M, Amos LA, Spillantini MG. Interaction of tau protein with the dynactin complex. Embo J. 2007; 26(21):4546–4554. [PubMed: 17932487]

47. Culver-Hanlon TL, Lex SA, Stephens AD, Quintyne NJ, King SJ. A microtubule-binding domain in dynactin increases dynein processivity by skating along microtubules. Nat Cell Biol. 2006; 8(3): 264–270. [PubMed: 16474384]
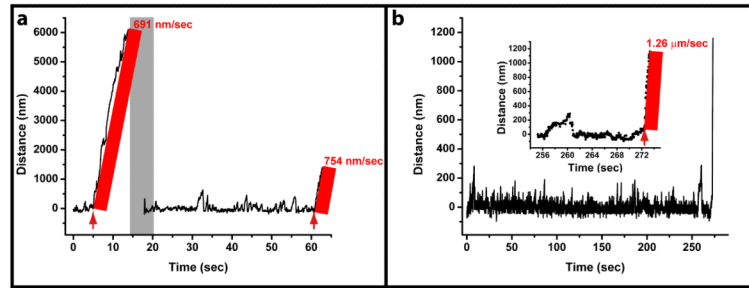
Fig. 1. Dynein shows robust motility in the optical trap
(a) A bead trapped in an 8 mW optical trap is brought near a bare MT and allowed to bind to the MT. At ~ 5 sec, the trap is turned off and motion of the bead along the MT is recorded. When the bead detaches from the MT, the optical trap is turned back on, the bead is recaptured, and again brought near a MT (the period of repositioning is highlighted in grey). The force production events are recorded for an extended period of time. After the recording, the bead is again released by turning the trap off (the times where the trap is turned off are shown by red arrows). The velocity before (~691 nm/sec) and after (~754 nm/sec) an extended period of the bead being in the trap are comparable. (b) A bead was trapped in a 28 mW optical trap (the power used for most data recording in this paper) for more than four minutes. Upon release (see inset for zoomed in portion of the track's end), the bead traveled at a high velocity (1.26 μm/sec). These results illustrate that dynein motors showed robust consistent characteristics, such as fast travel, even when exposed to an optical trap (as high as 28 mW) for several minutes.
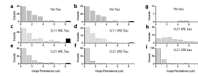
Fig.2. Tau's effect on dynein-based travel distances

Dynein-based travel for beads incubated at lower (panels a-f) and higher (panels g-i) dynein concentrations is shown. Parallel assays were used to compare transport on MTs with increasing amounts of tau. Panels a, c and e show the effect of increasing 4RL tau (0, ~0.1, ~0.2 tau/tubulin dimer, respectively). Similarly, panels b, d and f show the effect of increasing 3RS tau. For ease of comparison, the histogram for the no tau case is reproduced twice (a,b). Results for 4RL (c,e) and 3RS (d,f) tau isoforms show that the effect of tau on MTs only becomes significant at higher concentrations of either isoform, and that the 3RS isoform inhibits dynein-based transport more strongly. Similarly, at higher dynein concentrations (panels g-i) robust long-range dynein-based transport on bare MTs (g) is notably inhibited by ~0.2 tau/tubulin dimer of 4RL (h) and 3RS (i) isoforms. The 3RS isoform is again found to be the more potent inhibitor of transport. The black bars represent counts where the beads traveled beyond the field of view of the microscope. Exponential decay fits to the data in (a), (c), (d), (e), (f), (i) have decay lengths 2.23 ± 0.13; 2.21 ± 0.20; 1.77 ± 0.14; 1.38 ± 0.14; 0.59 ± 0.07; 0.84 ± 0.08 μm respectively (mean estimate from fit $\pm$ SEM). Statistical significance of differences in means of distributions was analyzed using ranksum test (95% confidence interval). The means of distributions in (a), (c), (d), (e) are not significantly different from each other but are significantly different from the distribution in (f). Interestigly, the mean decay length in (i) is significnatly larger than in (f), reflecting the increased number of motors present in (i). Elsewhere in the paper, data presented corresponds to the lower dynein concentration, panels a-f.
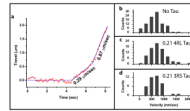
**Fig. 3. Tau's effect on dynein-based travel velocities**
(a) A sample track of dynein-based bead travel. In this case, once the bead is released from the trap, its motion consists of two constant velocity segments (least square fit is shown in blue and annotated with corresponding velocities). The histograms for velocity segments are shown for motion on bare MTs (b), MTs covered with ~0.2 4RL tau/tubulin dimer (c), and MTs covered with ~0.2 4RL tau/tubulin dimer (d). The distributions are peaked around 650 ± 31, 748 ± 39, 658 ± 44 nm/sec in panels (b), (c), and (d) respectively (mean ± SEM). The difference between the no tau and 4RL tau velocities is not statistically significant (ranksum test used due to presence of high velocity outliers, p=0.081). We observed no reproducible difference in velocities due to tau's presence on MTs.
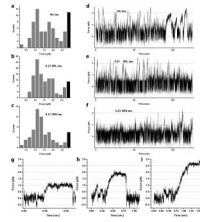
Fig. 4. Dynein force production in the presence of tau
Histograms of stalling forces with no tau on MTs (a), ~0.2 4RL tau/tubulin dimer (b), and ~0.2 3RS tau/tubulin dimer (c) feature three identifiable peaks (at ~1.1 pN, ~1.8 pN, and ~2.6 pN). The decrease in counts on the high-force side of the ~2.6 pN peak are not shown here (but see expanded histogram in supplement). Black bars represent counts for stall forces outside the linear range of the optical trap. Example stall shapes corresponding to the three peaks are shown in (g-i) respectively. Notably, higher stall force are significantly suppressed (but still observed) in the 3RS tau assay (c). Indeed, the reduction is also seen in overall force production (not just stall events). Representative bead displacement in an optical trap (panels d-f) for one bead is shown for each assay. The force production for no tau (d) and high 4RL tau (e) events are similar. The frequency of moderate and high force events in the high 3RS assay is significantly reduced (f). Because the motors need to move extremely short distances to generate such forces, this decrease reflects an effect of tau on the motor's on-rate, confirming the general picture derived from the stall-force histograms (a-c). We conclude that high amounts of 3RS tau can significantly reduce the average number of engaged motors in our dynein assay, but that multiple motors can still engage in transport.
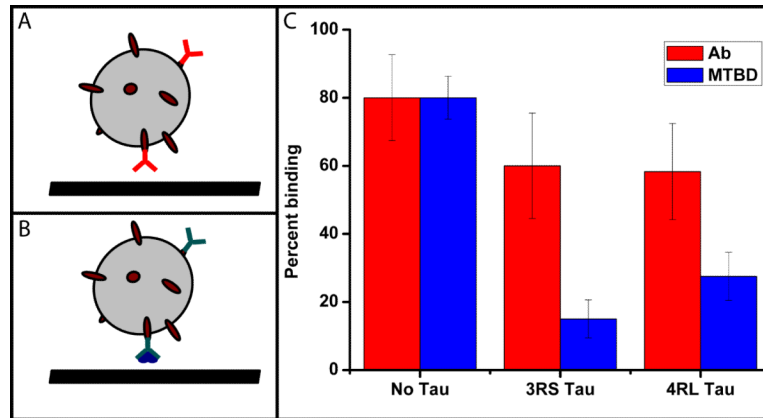
Fig. 5. Static binding experiments probe the role of tau at and away from the MT
We tested how tau affects binding of MTBD to MTs with bead-based assay (a,b). We used polystyrene beads (schematically represented by grey spheres) conjugated to protein A (dark red ovals). Protein A was in turn bound with anti-tubulin antibody (red Y) or anti-GST antibody (cyan Y) and GST-tagged MTBD of dynein (dark blue). These two bead configurations were bound to MTs with no tau, 3RS and 4RL tau (0.21 bound tau/tubulin dimer ratio). The results of binding experiments are shown in (c). The presence of either isoform of tau on MTs only slightly reduces bead binding to MTs (red bars). However, tau very strongly inhibits the binding of MTBD of dynein (blue bars) even though the geometries used (a,b) are nearly identical. Note that the 3RS inhibits MTBD binding more, consistent with our observation that this isoform has a stronger effect on dynein on-rate and dynein-driven bead travel distances (Fig. 2, 4). Note also that the full dynein motor has two binding domains so the net effect of tau on full motor binding is likely to be less pronounced than for a single dynein's MT-binding domain. The error bars shown are estimated as

$$\sqrt{P(1-P)/N_{\text{total}}},$$ where P is the fraction of binding events and N_{total} is the number of beads tested.